

Resonant excitation of strong plasma wakefields by relativistic electron microbunches

Xiao-Juan Wang(王晓娟), Hao Peng(彭浩), Tai-Wu Huang(黄太武), Zhang-Hu Hu(胡章虎), Ran Li(李然), Ke Jiang(蒋轲), Di-Kai Li(李迪开), Jian Yu(俞健), Ming-Yang Yu(郁明阳), Lei-Feng Cao(曹磊峰), Cang-Tao Zhou(周沧涛), Shuang-Chen Ruan(阮双琛)

Citation: Chin. Phys. B. 35, 095202 (2026). DOI: 10.1088/1674-1056/ae1cb5 |
CSTR: 32038.14.CPB.ae1cb5
http://cpb.iphy.ac.cn; http://iopscience.iop.org/cpb

What follows is a list of articles you may be interested in

Tunable energy spectrum betatron x-ray sources in a plasma wakefield

Chuan-Yi Xi(奚传易), Yin-Ren Shou(寿寅任), Li-Qi Han(韩立琦), Abdughupur Ablimit(阿卜杜伍普尔·阿布力米提), Xiao-Dan Liu(刘晓丹), Yan-Ying Zhao(赵研英), Jin-Qing Yu(余金清)
Chin. Phys. B. 33, 085202 (2024). DOI: 10.1088/1674-1056/ad4531

Effect of sharp vacuum–plasma boundary on the electron injection and acceleration in a few-cycle laser driven wakefield

Guo-Bo Zhang(张国博), Song Liu(刘松), De-Bin Zou(邹德滨), Ye Cui(崔野), Jian-Peng Liu(刘建鹏), Xiao-Hu Yang(杨晓虎), Yan-Yun Ma(马燕云), Fu-Qiu Shao(邵福球)
Chin. Phys. B. 32, 095202 (2023). DOI: 10.1088/1674-1056/acdc0c

Optimization of the beam quality in ionization injection by a tailoring gas profile

Ye Cui(崔野), Guo-Bo Zhang(张国博), Yan-Yun Ma(马燕云), Xiao-Hu Yang(杨晓虎), Jia-Yin Mu(牟佳胤), Hai-Bo Yao(姚海波), Ming Zi(资明), Jie Zhou(周洁), Jing-Qi Yang(杨静琦), Li-Xiang Hu(胡理想), Li-Chao Tian(田立朝)
Chin. Phys. B. 30, 105201 (2021). DOI: 10.1088/1674-1056/ac1b89

Nonlinear propagation of an intense Laguerre-Gaussian laser pulse in a plasma channel

Mingping Liu(刘明萍), Zhen Zhang(张震), Suhui Deng(邓素辉)
Chin. Phys. B. 30, 055204 (2021). DOI: 10.1088/1674-1056/abd68c

Acceleration and radiation of externally injected electrons in laser plasma wakefield driven by a Laguerre-Gaussian pulse

Zhong-Chen Shen(沈众辰), Min Chen(陈民), Guo-Bo Zhang(张国博), Ji Luo(罗辑), Su-Ming Weng(翁苏明), Xiao-Hui Yuan(远晓辉), Feng Liu(刘峰), Zheng-Ming Sheng(盛政明)
Chin. Phys. B. 26, 115204 (2017). DOI: 10.1088/1674-1056/26/11/115204

Resonant excitation of strong plasma wakefields by relativistic electron microbunches

Xiao-Juan Wang(王晓娟)[1,2], Hao Peng(彭浩)[2,†], Tai-Wu Huang(黄太武)[2,‡], Zhang-Hu Hu(胡章虎)[3], Ran Li(李然)[2], Ke Jiang(蒋轲)[2], Di-Kai Li(李迪开)[2], Jian Yu(俞健)[2], Ming-Yang Yu(郁明阳)[2], Lei-Feng Cao(曹磊峰)[2,§], Cang-Tao Zhou(周沧涛)[2], and Shuang-Chen Ruan(阮双琛)[2]

[1] *College of Applied Sciences, Shenzhen University, Shenzhen* 518060, *China*

[2] *Shenzhen Key Laboratory of Ultraintense Laser and Advanced Material Technology, Center for Intense Laser Application Technology, and College of Engineering Physics, Shenzhen Technology University, Shenzhen* 518118, *China*

[3] *School of Physics, Dalian University of Technology, Dalian* 116024, *China*

(Received 27 August 2025; revised manuscript received 1 November 2025; accepted manuscript online 7 November 2025)

We propose a self-consistent two-stage scheme for exciting ultra-high-gradient plasma wakefields via resonant interaction between a relativistic electron beam and plasmas. In the first stage, a low-density relativistic electron beam undergoes self-focusing and energy-chirp-induced betatron oscillations in an underdense plasma, spontaneously and self-consistently evolving into a train of periodic and dense microbunches. These *in-situ* formed microbunches are then injected into a denser plasma, where the microbunch period precisely matches the plasma wavelength, leading to resonant excitation of wakefields with peak amplitudes approaching 1 TV/m. Three-dimensional particle-in-cell (PIC) simulations confirm that microbunching periodicity matching the plasma wavelength is essential for maximizing the wakefield strength. By 'self-shaping' the driver beam, our scheme significantly relaxes initial beam requirements, enhancing its robustness and feasibility for next-generation plasma accelerators.

Keywords: relativistic electron microbunches, plasma wakefield, resonant excitation, particle-in-cell simulation

PACS: 52.35.Hr, 94.20.wf, 29.27.–a, 41.75.Ht

DOI: 10.1088/1674-1056/ae1cb5 **CSTR:** 32038.14.CPB.ae1cb5

1. Introduction

Plasma-based accelerators have emerged as a highly promising paradigm for next-generation particle accelerators, offering accelerating gradients of 10 GV/m to 100 GV/m, which surpass conventional radio-frequency systems by orders of magnitude.[1–5] This remarkable capability holds the potential to drastically reduce the size and cost of future TeV colliders and compact x-ray free-electron lasers.[6–8] Traditionally, achieving such extreme gradients can be achieved by a single, short electron bunch with a length much smaller than the plasma wavelength ($L_{\rm bunch} \ll \lambda_{\rm p}$) and high charge density.[5,9,10]

To circumvent the stringent requirements of single-bunch drivers, the concept of resonant excitation offers a compelling alternative. By employing periodic electron microbunches, the wakefield can be coherently amplified when the bunch spacing matches the plasma wavelength, dramatically enhancing the total field strength.[11–14] Various techniques have successfully generated such microbunch trains, including inverse free electron lasers (IFEL)[15–18] and masking techniques.[11,19,20] For example, experiments demonstrate that after ultraviolet laser irradiation of a copper cathode and acceleration to 95 MeV via an RF linac, the resulting electron microbunches can resonantly excite strong wakefields in underdense plasma. However, these approaches almost invariably rely on complex external devices and precise external synchronization, which complicates experimental setups and limits their scalability and robustness. To reduce such external dependencies, researchers have explored intrinsic beam-plasma instabilities, most notably the self-modulation instability (SMI), to transform long particle bunches into microbunch trains within the plasma itself.[21–24]

In this work, we present a fundamentally different approach that exploits the intrinsic self-organization capabilities of relativistic electron beams (REBs) in plasma. A two-stage method is proposed to generate ultra-high gradient plasma wakefields through resonant excitation by relativistic electron microbunches without requiring external synchronization or ancillary devices. In the first stage (stage I), an REB undergoes self-focusing in an underdense plasma and develops asynchronous envelope oscillations, leading to the autonomous formation of microbunches with precisely controlled spacing. In the second stage (stage II), the self-organized structure then

†Corresponding author. E-mail: penghao@sztu.edu.cn

‡Corresponding author. E-mail: taiwu.huang@sztu.edu.cn

§Corresponding author. E-mail: caoleifeng@sztu.edu.cn

© 2026 Chinese Physical Society and IOP Publishing Ltd. All rights, including for text and data mining, AI training, and similar technologies, are reserved.

enters a relatively denser plasma where the microbunch periodicity can be matched to the denser plasma wavelength, enabling optimal resonant excitation. Through this two-stage method, we can efficiently generate ultra-high gradient plasma wakefields, opening up a new path for the development of plasma wakefield accelerators.

2. Simulation method

To validate the feasibility and underlying physics of the proposed scheme, we perform three-dimensional (3D) particle-in-cell (PIC) simulations using the FBPIC code[25] to systematically study the beam dynamics in both plasma stages. The solver of FBPIC employs the spectral quasi-cylindrical Pseudo-Spectral Analytical Time Domain (PSATD) solver to integrate Maxwell's equations in the frequency domain. This approach enables high-precision derivative calculation and dispersion-free performance in all directions, effectively avoiding numerical artifacts. The simulation setup consists of two distinct stages: (i) The REB enters the underdense plasma region, where microbunches form via beam self-focusing and asynchronous betatron oscillations in the self-driven wakefield; (ii) These microbunches are subsequently injected into the relatively denser plasma, with its density carefully chosen to match the plasma wavelength with the microbunch periodicity, thereby achieving resonant excitation. Specifically, the density distribution and length parameters of each plasma stage are defined as follows: the underdense plasma in stage I has a fixed density of 10^{25} m^{-3} with a length of $1200c/\omega_{\rm pe}$, while the relatively denser plasma in stage II is adjusted to a density of 10^{27} m^{-3}. From the perspective of current technology, experiments have achieved background plasmas with near-critical density.[5,26] To simplify the simulation setup, we directly constructed a density-graded plasma between stage I and stage II in the simulation model. In experiments, several schemes have been proposed to generate such density transitions.[27–29]

In the simulations, one azimuthal electromagnetic mode is utilized, and the number of particles per cell along the longitudinal, radial, and azimuthal directions is set to $N_z \times N_{\rm r} \times N_\theta = 2 \times 2 \times 8$. The grid size is $\lambda_{\rm p}/200$ in both the longitudinal (*i.e.*, along the REB propagation direction) and transverse directions. Here, $\lambda_{\rm p} = 2\pi c/\omega_{\rm pe}$ is the plasma wavelength, where c is the speed of light in vacuum, $\omega_{\rm pe} = \sqrt{n_{\rm pe0}e^2/m_{\rm e}\varepsilon_0}$ is the plasma frequency based on the underdense plasma density $n_{\rm pe0} = 10^{25}$ m^{-3}, $-e$ and $m_{\rm e}$ are the electron charge and mass, and ε_0 is the vacuum permittivity. The simulation results remain consistent when calculations are performed using a smaller grid size, verifying the accuracy of the simulation results.

Unless otherwise stated, the initial parameters of the input REB are: density $n_{\rm be0} = 10^{24}$ m^{-3}, normalized emittance $\varepsilon_{\rm N} = 0.5$ μm, mean Lorentz factor $\gamma = 200$, and energy spread $\Delta E/E = 1\%$. The initial REB has a Gaussian profile with length $\sigma_z = \lambda_{\rm p}/2$ and radius $\sigma_{\rm r} = \lambda_{\rm p}/\pi$. Such electron beams are experimentally achievable through laser–plasma interactions or conventional accelerators. Currently, plasma wakefield accelerators can produce high-energy electron beams on the order of hundreds of MeV with energy spread less than 1% and normalized emittance below 1 μm.[20,30–32] For the timescales of interest in this study, the motion of plasma ions is neglected. We focus on the evolution of the REB, for which the moving window technique proved to be a simpler and more effective method. In the simulations, we employ a moving window with the speed of light in vacuum c and longitudinal coordinate $\xi = z - ct$. Importantly, in our scheme, the REB length must be smaller than the plasma wavelength ($\sigma_z \leq \lambda_{\rm p}$) to avoid modulation instability and ensure controlled formation of microbunches, which are subsequently injected into the relatively denser plasma. Conversely, if the length of the REB is larger than the plasma wavelength ($\sigma_z \gg \lambda_{\rm p}$), the SMI longitudinally breaks up the beam on the scale of the plasma wavelength $\lambda_{\rm p}$.[21–24]

3. Bunching of REB in its self-driven plasma wakefield

In the first stage, an REB is injected into plasma and generates a linear plasma wakefield. Simultaneously, the transverse focusing force of this wakefield induces beam self-focusing, leading to transverse compression and a significant increase in beam density.[33,34] This process operates through a positive feedback mechanism: as beam density increases, the wakefield focusing gradient strengthens, which further accelerates beam compression. As the beam density approaches or exceeds the underdense plasma density, the REB completely expels background plasma electrons from its path, forming a plasma bubble. This process excites a nonlinear plasma wakefield that imparts linear transverse focusing forces and generates a longitudinally inhomogeneous accelerating gradient (Fig. 1(b)), ultimately leading to the development of an energy chirp throughout the REB. The transverse wakefield compresses the REB into a filament and induces betatron oscillations with the frequency of $\omega_\beta = \omega_{\rm pe}/\sqrt{2\gamma}$. This energy chirp causes variations in betatron oscillation frequency among electrons at different longitudinal positions within the REB. These energy-dependent betatron oscillations lead to progressive phase dispersion of the transverse oscillations, resulting in longitudinal modulation of the beam envelope. Specifically, regions of envelope contraction (peak focusing) correspond to electron density maxima (forming microbunch cores), while envelope expansion yields density minima.[35] As a result, this process ultimately leads to periodic microbunch formation via three-dimensional modulation, as displayed in Fig. 1(a).

These microbunches are characterized by a peak density of 1.5×10^{26} m^{-3} and a tunable spacing of $\Delta\xi = 1$ μm. Crucially, we have deduced that the microbunching spacing can be precisely controlled by tuning two key parameters: the initial energy of the REB (characterized by its Lorentz factor γ_0) and the propagation time (t') of the REB within the self-driven plasma bubble. This controllable spacing follows the relationship:[36] $\Delta\xi \sim 4\pi\sqrt{2\gamma_0}\alpha c\gamma_0/\omega_{pe}^3 t'^2$, where $\alpha = 10$ is a fitting constant associated with the beam-driven wakefield gradient.[37] By optimizing the initial parameters of the REB and plasma in this first stage, the periodicity of the self-formed microbunches can be accurately controlled, allowing for precise matching with the denser plasma wavelength for subsequent resonant excitation.

4. Resonant excitation in the relatively denser plasma

After the REB forms periodic microbunches with precisely controlled spacing $\Delta\xi$ in the underdense plasma, these microbunches are injected into a carefully tuned relatively denser plasma. The density of this second-stage plasma is adjusted to satisfy the resonance condition: $\lambda_D \approx \Delta\xi$, where λ_D denotes the denser plasma wavelength. Under these conditions, each microbunch excites a plasma oscillation at the denser plasma frequency ω_D. Importantly, each subsequent microbunch arrives at the optimal phase of the preceding wakefield. This precise synchronization ensures that the wakefields generated by successive microbunches undergo coherent constructive interference along the propagation axis, leading to significant enhancement of the overall wakefield amplitude. As a concrete example, once the periodic microbunches with $\Delta\xi = 1$ μm are formed (Fig. 1(a)), they are injected into a relatively denser plasma with density of 10^{27} m^{-3} (Fig. 1(d)), corresponding to the dense plasma wavelength $\lambda_D = 1$ μm. Under such resonant conditions, the wakefield amplitude is amplified to approach 1 TV/m via resonant excitation,[18] as displayed in Fig. 1(e).

To directly verify the resonant excitation of plasma waves, we perform Fourier analysis of the longitudinal wakefield E_z along the beam axis in the denser plasma region (stage II). As shown in the blue solid line of Fig. 1(f), the spectrum exhibits a sharp and dominant peak at the plasma wavenumber k_D corresponding to the denser plasma density. We analyze the quality of microbunch periodicity using the bunching factor $b(k) \equiv \left|\sum_{j=1}^{N} \exp(ikz_j)\right|/N$, which has a maximum theoretical value of unity.[38,39] Here z_j is the longitudinal position of the electron j, N is the total number of electrons involved, and k refers to the wave number. For perfectly periodic microbunches with spacing $\Delta\xi$, their bunching factor $b(k)$ peaks at wavenumber $k = 2\pi/\Delta\xi$. As shown in Fig. 1(f), the dominant wavenumbers in both the bunching factor and the wakefield Fourier spectrum are identical. This direct alignment confirms that the microbunch spacing matches the denser plasma wavelength, thereby unequivocally validating the successful resonant excitation of plasma oscillations.

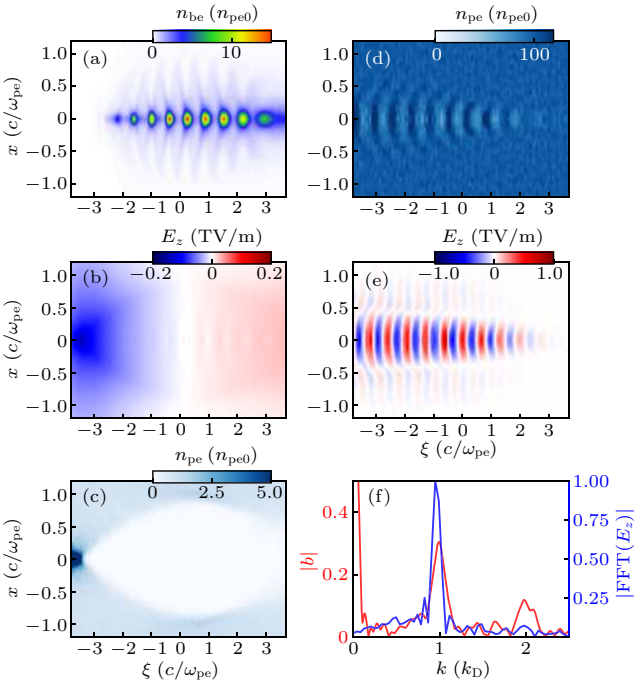


Fig. 1. The formation of microbunches by REB in underdense plasma with density 10^{25} m^{-3} (stage I, (a)–(c)), and the excitation of stronger plasma wakefields as microbunches enter denser plasma with density of 10^{27} m^{-3}(stage II, (d)–(e)) are shown. The distributions of REB density n_{be}(a), longitudinal wakefield E_z ((b) and (e)), and plasma electron density n_{pe} ((c) and (d)) at $t = 1200\omega_{pe}^{-1}$ (stage I) and $t = 1220\omega_{pe}^{-1}$ (stage II) are displayed. The bunching factor (red solid line) of these microbunches within a radius of $0.25\omega_{pe}$ at $t = 1200\omega_{pe}^{-1}$ and Fourier analysis of the longitudinal axis in the longitudinal wakefield E_z (blue solid line) at t = $1220\omega_{pe}^{-1}$ are also shown in Fig. 1(f).

5. Effect of microbunches' periodicity on resonance conditions

To elucidate the critical role of structural periodicity and its precise matching to the plasma wavelength in wakefield amplification, we conduct comparative simulations between non-periodic dense current filaments and periodic microbunches. First, we examine the non-periodic case, where an REB self-focuses into a dense current filament (microbunches are not formed). Although this filament excites wakefields upon injection into the denser plasma, the maximum longitudinal field is only 0.1 TV/m, as shown in Fig. 2(a). This field strength is significantly lower than 1 TV/m achieved by periodic microbunches, as observed in Fig. 1(e). The underlying mechanism for this discrepancy is the absence of periodicity, resulting in an extremely low bunching factor at the denser plasma frequency (Fig. 2(b)). Consequently, the non-periodic structure cannot support the coherent superposition of wakefields, thereby directly confirming that periodicity is a necessary condition for resonant excitation.

Next, to further validate the importance of matching between microbunch spacing and plasma wavelength, we simulate a case where the microbunch spacing deliberately deviates from the plasma wavelength. After propagating approximately 1003 c/ω_{pe} in an underdense plasma, the REB self-organizes into microbunches with a period of 1.5 μm. When these microbunches are injected into a denser plasma with a shorter wavelength of $\lambda_D = 1$ μm, the resulting wakefield amplitude reaches only 0.2 TV/m. The bunching factor reaches a peak at a wavenumber of $0.67k_D$ (corresponding to the wavelength 1.5 μm), indicating a mismatch with the plasma wavelength (Fig. 2(d)). The deviation of the bunching factor peak from the plasma's intrinsic wavenumber further demonstrates that even with periodicity, mismatched spacing significantly attenuates the resonant effect.

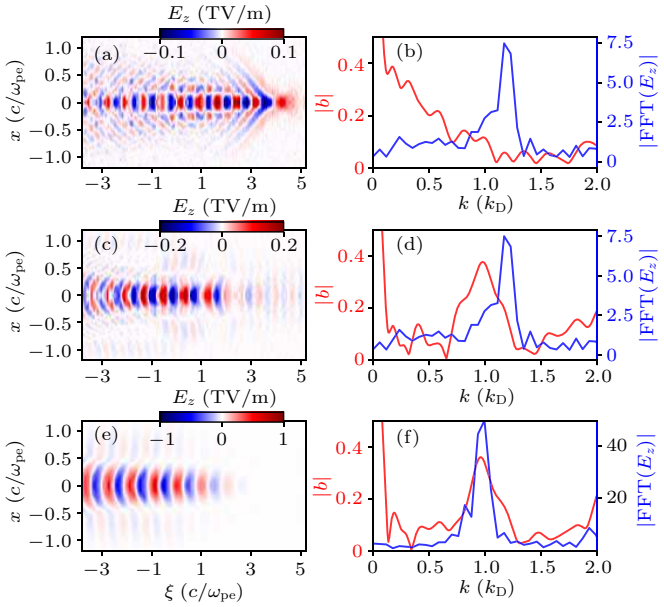


Fig. 2. Comparison of wakefields excited by non-periodic electron filaments and periodic microbunches ($\Delta\xi = 1.5$ μm) formed at $t = 1003\omega_{pe}^{-1}$ in underdense plasma ($n_{pe} = 10^{25}$ m^{-3}). Non-periodic filaments ((a)–(b)): Longitudinal wakefield E_z (a) at $t = 178\omega_{pe}^{-1}$ in the dense plasma ($n_{pe} = 10^{27}$ m^{-3}); (b) The bunching factors (red solid line) of these beam electrons within a radius of $0.25\omega_{pe}$ and Fourier analyses of the longitudinal axis in the E_z (blue solid line); Periodic microbunches in mismatched plasma with $n_{pe} = 10^{27}$ m^{-3} ((c)–(d)): E_z at $t = 1021\omega_{pe}^{-1}$ (c) and (d) corresponding bunching factors (red solid line) and Fourier analyses of the longitudinal axis in the E_z (blue solid line); Periodic microbunches in matched plasma with $n_{pe} = 5\times10^{26}$ m^{-3} ((e)–(f)): E_z at $t = 1021\omega_{pe}^{-1}$(e) and (f) corresponding bunching factors (red solid line) and Fourier analyses of the longitudinal axis in the E_z (blue solid line).

Finally, resonant excitation can be restored by adjusting the plasma wavelength to match the microbunch spacing. To demonstrate this, we consider an REB that self-modulates into microbunches with a fixed period of 1.5 μm. These microbunches are then injected into denser plasma with a density of $n_D = 5\times10^{26}$ m^{-3}, specifically chosen to yield a matching plasma wavelength of $\lambda_D = 1.5$ μm, thereby satisfying the resonance condition ($\Delta\xi = \lambda_D$). Under this precise resonance condition, the primary peak of the bunching factor aligns perfectly with the Fourier spectrum of the plasma wakefield E_z, as illustrated in Fig. 2(f). As a direct consequence, the wakefield amplitude is restored to a strong 1 TV/m (Fig. 2(e)), which is in excellent agreement with the theoretical resonance condition and consistent with our previous resonant case (Figs. 1(e) and 1(f)). Notably, once resonance is achieved, the peak wakefield amplitude becomes largely insensitive to the number of microbunches (see Fig. 1(e)). This is consistent with the saturation effect in resonant wakefield excitation, where the wakefield approaches the wave-breaking limit after a sufficient number of driver bunches.[40]

In summary, these findings unequivocally demonstrate that both the intrinsic periodicity of microbunches and the precise matching between their spacing and the denser plasma wavelength are critical for maximizing wakefield amplification. This provides a quantitative basis for optimizing experimental parameters to achieve ultra-high gradient plasma wakefields.

6. Impact of beam charge and emittance

In addition to the periodicity and wavelength-matching conditions, the intrinsic beam parameters, particularly charge and emittance, play a decisive role in determining whether microbunches can form and how strong the resonantly excited wakefields can become. From the envelope oscillation equation and the conditions for exciting nonlinear plasma wakefields, the condition for stable microbunching can be expressed as:[36] $\tilde{\varepsilon}_N \lesssim \tilde{\sigma}_r{}^2\tilde{n}_{be}\sqrt{\gamma/2}$, where $\tilde{\sigma}_r$ and $\tilde{\varepsilon}_N$ denote the normalized initial radius and emittance with respect to the plasma skin depth, and $\tilde{n}_{be} = n_{be0}/n_{pe0}$ is the ratio of the initial REB density to the underdense plasma density. Note that the product $\tilde{\sigma}_r{}^2\tilde{n}_{be}$ is proportional to the beam charge. Thus, this relation highlights that both beam charge and emittance are the key control parameters for microbunch formation and subsequent wakefield excitation. Meanwhile, it is noted that the beam energy also determines the process of microbunch formation, but has little effect on the strength of the excited wakefield.

We first investigate how varying the initial beam charge modifies the resonant excitation process. For the large-charge case ($\tilde{n}_{be} = 0.1$ and $\tilde{\sigma}_r = 2$), the REB readily self-organizes into microbunches, which resonantly drive plasma oscillations with a peak wakefield amplitude up to 1 TV/m (Fig. 2(e)). In the moderate-charge case ($\tilde{n}_{be} = 0.05$ and $\tilde{\sigma}_r = 2$), the condition of microbunching is still satisfied, and thus the REB still forms microbunches with a periodicity of 1.5 μm, as displayed in Figs. 3(a) and 3(c). However, the resulting wakefield amplitude drops drastically to only 0.2 TV/m (Fig. 3(b)). Finally, for the low-charge case ($\tilde{n}_{be} = 0.025$ and $\tilde{\sigma}_r = 2$), the condition of microbunching is not satisfied, thus the REB only undergoes transverse self-focusing without forming microbunches, as illustrated in Fig. 3(d). This density of REB is lower than the dense plasma density, resulting in a negligible excited plasma

wakefield (Fig. 3(e)). These results establish that beam charge primarily governs the magnitude of resonantly excited wakefields: higher charge directly leads to stronger fields, while insufficient charge suppresses microbunch formation altogether.

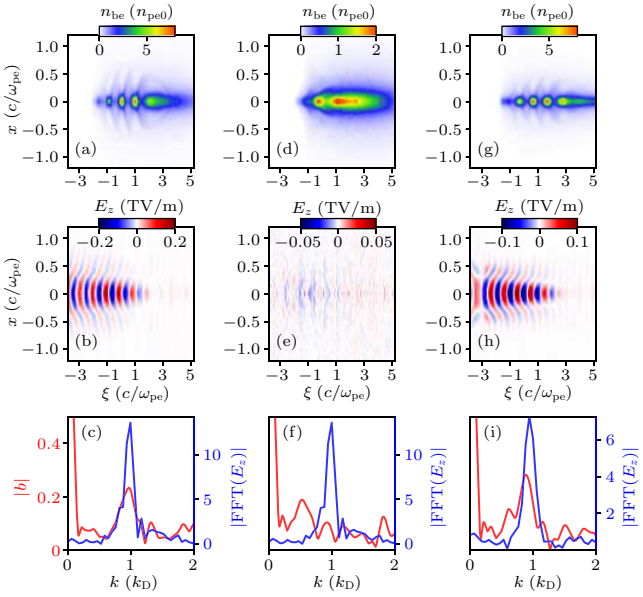


Fig. 3. Comparison of wakefields for the moderate-charge case ((a)–(c)) $\tilde{n}_{be} = 0.05$, $\tilde{\sigma}_r = 2$, and $\varepsilon_N = 0.5$ μm, low-charge case ((d)–(f)) $\tilde{n}_{be} = 0.025$, $\tilde{\sigma}_r = 2$, and $\varepsilon_N = 0.5$ μm, low-emittance case ((g)–(i)) $\tilde{n}_{be} = 0.1$, $\tilde{\sigma}_r = 1$, and $\varepsilon_N = 0.1$ μm. Density distribution of the REB n_{be} ((a), (d), and (g)) with moderate-charge at $t = 1306\omega_{pe}^{-1}$ (a), with low-charge at $t = 1603\omega_{pe}^{-1}$ (d), and with low emittance at $t = 1603\omega_{pe}^{-1}$ (g) in underdense plasma. Longitudinal wakefield E_z ((b), (e), and (h)) with moderate-charge at $t = 1319\omega_{pe}^{-1}$ (b), with low-charge at $t = 1616\omega_{pe}^{-1}$(e), and with low emittance at $t = 1616\omega_{pe}^{-1}$ (h) in denser plasma. The bunching factors (red solid line) for the microbunches within a radius of $0.25\omega_{pe}$ are shown. Fourier analysis of the longitudinal axis in the E_z (blue solid line) are also shown in (c), (f), and (i). The density of denser plasma is $n_D = 5 \times 10^{26}$ m^{-3}.

Next, we explore the role of beam emittance, which determines the ability of the beam to maintain tight focusing and form microbunches. For the relatively high emittance (low-charge) case ($\varepsilon_N = 0.5$ μm, $\tilde{n}_{be} = 0.025$, and $\tilde{\sigma}_r = 2$), the beam divergence reduces the efficiency of microbunch formation and the strength of wakefield excitation (Figs. 3(d) and 3(e)). Notably, another case with identical emittance but different $\tilde{n}_{be}$ and $\tilde{\sigma}_r$ ($\varepsilon_N = 0.5$ μm, $\tilde{n}_{be} = 0.1$, $\tilde{\sigma}_r = 1$; results not shown here) shows simulation results nearly identical to the low-charge case ($\varepsilon_N = 0.5$ μm, $\tilde{n}_{be} = 0.025$, and $\tilde{\sigma}_r = 2$). Both share the same low charge, leading to only focusing—no microbunch formation or strong wakefield generation. By contrast, in the low-emittance case ($\varepsilon_N = 0.1$ μm, $\tilde{n}_{be} = 0.1$, and $\tilde{\sigma}_r = 1$) with the same low charge as the above cases, the REB preserves tight focusing and still produces periodic microbunches with a bunching factor of about 0.25, as shown in Figs. 3(g) and 3(i). It is noted that although low emittance can improve microbunch quality, it cannot replace the role of charge in generating strong wakefields. As seen in Figs. 3(h) and 3(i), even with low emittance, the wakefield amplitude remains limited to 0.1 TV/m.

The systematic comparison reveals two distinct roles: (i) beam charge is the dominant factor controlling the wakefield amplitude, as it directly determines the strength of the plasma response; (ii) emittance mainly influences the efficiency of microbunch formation by regulating the transverse beam quality. Therefore, achieving strong resonant excitation requires both adequate charge to drive intense plasma oscillations and sufficiently low emittance to sustain periodic microbunching. From an experimental perspective, one should prioritize maintaining large beam charge while minimizing emittance, thereby maximizing both the strength and stability of the wakefield. Currently, the core challenge for implementing in experiments lies in the precise matching between microbunches periodicity and plasma wavelength in stage II. However, with the development of beam and plasma technology, we believe that the controllability and feasibility of experiments would be continuously improved, enabling the current experimental difficulties to be sufficiently overcome.

Finally, it should be mentioned that scenarios with higher energy or lower plasma density would require significantly longer times to capture the complete microbunching process, which directly amplifies computational costs. Theoretically, this mechanism can be extended to cases with higher beam energy or lower plasma density, which allows the resonantly excited wakefield to persist over a longer time scale, beneficial to the acceleration of charged particles.

7. Conclusion

The two-stage scheme proposed in this study successfully excites ultra-high-gradient wakefields with amplitudes approaching 1 TV/m in relatively denser plasma through the self-organization of REB. The autonomous formation of microbunches via energy-dependent betatron oscillations, coupled with their resonant interaction with relatively denser plasma, enables acceleration gradients approaching 1 TV/m. Our comprehensive simulations demonstrate that precise alignment of microbunch spacing with the plasma wavelength amplifies wakefield amplitudes, producing electric fields far surpassing those of conventional beam-driven systems. This two-stage scheme not only offers a more robust solution for next-generation plasma accelerators but also enhances the flexibility of accelerator designs by reducing the strict requirements on the initial beam. Specifically, experimental setups can optimize the initial density, energy, and emittance of the REB to fine-tune the microbunch spacing and match it with various plasma conditions. Moreover, this approach holds significant potential for applications in compact particle accelerators and high-energy-density plasma research. Future research can focus on integrating this method with existing accelerator systems, exploring ways to validate its effectiveness in large-scale experiments, and evaluating its scalability for different experimental setups.

Acknowledgements

Project supported by the National Key Research and Development Program of China (Grant No. 2024YFA1613400), the National Natural Science Foundation of China (Grant Nos. 12475238, 12175154, 12205201, and 12475248), the Financial Support for Outstanding Talents Training Fund in Shenzhen (Project No. 202101), the Shenzhen Science and Technology Program (Grant No. RCYX20221008092851073), the Guangdong Province Key Construction Discipline Scientific Research Capacity Improvement Project (Grant No. 2021ZDJS107), the Natural Science Foundation of Guangdong Province, China (Grant No. 2025A1515012853), the Natural Science Foundation of Top Talent of SZTU (Grant Nos. GDRC202310 and GDRC202423), and the Guangdong Basic and Applied Basic Research Foundation (Grant No. 2025A1515010791).

References

[1] Chen P, Su J J, Dawson J M, Bane K L F and Wilson P B 1986 *Phys. Rev. Lett.* **56** 1252
[2] Tajima T and Dawson J M 1979 *Phys. Rev. Lett.* **43** 267
[3] Knetsch A, Andriyash I A, Gilljohann M, Kononenko O, Matheron A, Mankovska Y, San Miguel Claveria P, Zakharova V, Adli E and Corde S 2023 *Phys. Rev. Lett.* **131** 135001
[4] Picksley A, Stackhouse J, Benedetti C, Nakamura K, Tsai H E, Li R, Miao B, Shrock J E, Rockafellow E, Milchberg H M, Schroeder C B, van Tilborg J, Esarey E, Geddes C G R and Gonsalves A J 2024 *Phys. Rev. Lett.* **133** 255001
[5] Lindstrøm C A, Corde S, D'Arcy R, Gessner S, Gilljohann M, Hogan M J and Osterhoff J 2025 arXiv (Preprint 2504.05558v1)
[6] Wang W, Feng K, Ke L, Yu C, Xu Y, Qi R, Chen Y, Qin Z, Zhang Z, Fang M, Liu J, Jiang K, Wang H, Wang C, Yang X, Wu F, Leng Y, Liu J, Li R and Xu Z 2021 *Nature* **595** 516
[7] Pompili R, Alesini D, Anania M P, *et al.* 2022 *Nature* **605** 659
[8] Galletti M, Assmann R, Couprie M E, Ferrario M, Giannessi L, Irman A, Pompili R and Wang W 2024 *Nat. Photon.* **18** 780
[9] Chen P, Dawson J M, Huff R W and Katsouleas T 1985 *Phys. Rev. Lett.* **54** 693
[10] Roussel R, Andonian G, Lynn W, Sanwalka K, Robles R, Hansel C, Deng A, Lawler G, Rosenzweig J B, Ha G, Seok J, Power J G, Conde M, Wisniewski E, Doran D S and Whiteford C E 2020 *Phys. Rev. Lett.* **124** 044802
[11] Muggli P, Yakimenko V, Babzien M, Kallos E and Kusche K P 2008 *Phys. Rev. Lett.* **101** 054801
[12] Muggli P, Allen B, Yakimenko V, Fedurin M, Kusche K and Babzien M 2010 *AIP Conf. Proc.* **1299** 495
[13] Cowley J, Thornton C, Arran C, Shalloo R J, Corner L, Cheung G, Gregory C D, Mangles S P D, Matlis N H, Symes D R, Walczak R and Hooker S M 2017 *Phys. Rev. Lett.* **119** 044802
[14] Ross A J, Chappell J, van de Wetering J J, Cowley J, Archer E, Bourgeois N, Corner L, Emerson D R, Feder L, Gu X J, Jakobsson O, Jones H, Picksley A, Reid L, Wang W, Walczak R and Hooker S M 2024 *Phys. Rev. Res.* **6** L022001
[15] Kallos E, Muggli P, Katsouleas T, Yakimenko V, Stolyarov D, Pogorelsky I, Pavlishin I, Kusche K, Babzien M, Ben-Zvi I and Kimura W D 2006 *AIP Conf. Proc.* **877** 520
[16] Duris J, Li S, Driver T, *et al.* 2020 *Nat. Photon.* **14** 30
[17] Manwani P, Hansel C, Majernik N, Rosenzweig J and Yadav M 2021 *Proceedings of the* 12*th International Particle Accelerator Conference* **IPAC2021**
[18] Manwani P, Majernik N, Yadav M, Hansel C and Rosenzweig J B 2021 *Phys. Rev. Accel. Beams* **24** 051302
[19] Muggli P, Allen B, Yakimenko V, Fedurin M, Kusche K and Babzien M 2010 *AIP Conf. Proc.* **1299** 495
[20] Verra L, Galletti M, Biagioni A, *et al.* 2025 *Research Square* **2025** 6115160
[21] Kumar N, Pukhov A and Lotov K 2010 *Phys. Rev. Lett.* **104** 255003
[22] Okhotnikov N V and Lotov K V 2025 *Phys. Plasmas* **32** 033102
[23] Turner M, Walter E, Amoedo C, *et al.* 2025 *Phys. Rev. Lett.* **134** 155001
[24] Farmer J P and Della Porta G Z 2025 *Phys. Rev. Res.* **7** L012055
[25] Lehe R, Kirchen M, Andriyash I A, Godfrey B B and Vay J L 2016 *Comput. Phys. Commun.* **203** 66
[26] Wang X J, Hu Z H and Wang Y N 2020 *Phys. Rev. E* **101** 043203
[27] Wu Y, Yu C, Qin Z, Wang W, Zhang Z, Qi R, Feng K, Ke L, Chen Y, Wang C, Yang X, Leng Y, Liu J, Li R and Xu Z 2019 *Appl. Sci.* **9**
[28] Ke L, Yu C, Feng K, Qin Z, Jiang K, Wang H, Luan S, Yang X, Xu Y, Leng Y, Wang W, Liu J and Li R 2021 *Appl. Sci.* **11**
[29] Chang Y Y, Cabadağ J C, Debus A, Ghaith A, LaBerge M, Pausch R, Schöbel S, Ufer P, Schramm U and Irman A 2023 *Phys. Rev. Appl.* **20** L061001
[30] Wang W T, Li W T, Liu J S, Zhang Z J, Qi R, Yu C H, Liu J Q, Fang M, Qin Z Y, Wang C, Xu Y, Wu F X, Leng Y X, Li R X and Xu Z Z 2016 *Phys. Rev. Lett.* **117** 124801
[31] Zhongtao X, Changhai Y, Zhiyong Q, Xuhui J, Jiahui C, Qiaoxuan Z, Gatie A, Jianghua J, Ya H, Jintan C and Jiansheng L 2024 *Matter and Radiation at Extremes* **9** 035201
[32] Winkler P, Trunk M, Hübner L, Martinez De La Ossa A, *et al.* 2025 *Nature* **640** 907
[33] Hu Z H, Wang X J, Hui D X, Zhao Q T, Cheng R, Zhao Y T, Zhang Z M and Wang Y N 2020 *Phys. Plasmas* **27** 023103
[34] Wang X J, Hu Z H and Wang Y N 2022 *Plasma Sci. Technol.* **24** 025001
[35] Bulanov S V, Mourou G and Tajima T 2008 *Phys. Lett. A* **372** 4813
[36] Wang X J, Peng H, Huang T W, Hu Z H, Li R, Jiang K, Li D K, Yu J, Ye H X, Yu M Y, Cao L F, Zhou C T and Ruan S C 2025 *Matter and Radiation at Extremes* **10** 057203
[37] Golovanov A, Kostyukov I Y, Pukhov A and Malka V 2023 *Phys. Rev. Lett.* **130** 105001
[38] Jia Q K 2008 *Appl. Phys. Lett.* **93** 141102
[39] Xu X L, Li F, Tsung F S, Miller K, Yakimenko V, Hogan M J, Joshi C and Mori W B 2022 *Nat. Commun.* **13** 3364
[40] Kallos E, Katsouleas T, Kimura W D, Kusche K, Muggli P, Pavlishin I, Pogorelsky I, Stolyarov D and Yakimenko V 2008 *Phys. Rev. Lett.* **100** 074802